Extracellular production of tellurium nanoparticles by thephotosynthetic bacterium *Rhodobacter capsulatus*

Roberto Borghese[a,*], Marco Brucale[b], Gianuario Fortunato[a], Massimiliano Lanzi[c], Alessio Mezzi[b], Francesco Valle[d], Massimiliano Cavallini[d], Davide Zannoni[a]

[a] *Dept. of Pharmacy and Biotechnology, University of Bologna, Italy*
[b] *Institute for the Study of Nanostructured Materials (CNR-ISMN), Rome, Italy*
[c] *Dept. of Industrial Chemistry "Toso Montanari", University of Bologna, Italy*
[d] *Institute for the Study of Nanostructured Materials (CNR-ISMN), Bologna, Italy*

Abstract

The toxic oxyanion tellurite (TeO_3^{2-}) is acquired by cells of *Rhodobacter capsulatus* grown anaerobically in the light, *via* acetate permease ActP2 and then reduced to Te^0 in the cytoplasm as needle-like black precipitates. Interestingly, photosynthetic cultures of *R. capsulatus* can also generate Te^0 nanoprecipitates (TeNPs) outside the cells upon addition of the redox mediator lawsone (2-hydroxy-1,4-naphtoquinone). TeNPs generation kinetics were monitored to define the optimal conditions to produce TeNPs as a function of various carbon sources and lawsone concentration. We report that growing cultures over a 10 days period with daily additions of 1 mM tellurite led to the accumulation in the growth medium of TeNPs with dimensions from 200 up to 600–700 nm in length as determined by atomic force microscopy (AFM). This result suggests that nucleation of TeNPs takes place over the entire cell growth period although the addition of new tellurium Te^0 to pre-formed TeNPs is the main strategy used by *R. capsulatus* to generate TeNPs outside the cells. Finally, X-ray photoelectron spectroscopy (XPS) and Fourier transform infrared (FT-IR) analysis of TeNPs indicate they are coated with an organic material which keeps the particles in solution in aqueous solvents.

Introduction

Tellurium (Te) is a metalloid, which belongs to the Group 16 of the periodic table, sometimes referred to as chalcogens, which also includes oxygen (O), sulfur (S), selenium (Se) and polonium (Po). Normally, tellurium associates with other metals such as the telluride of gold, calaverite ($AuTe_2$), or silver/gold, sylvanite ($AgAuTe_4$). As Te shows strong metal like properties, it can exist in a number of redox states, namely: telluride (Te^{-II}) metal tellurium (Te^0) tellurite (Te^{IV}) tellurate (Te^{VI}).

Prokaryotes and eukaryotes face tellurium mainly in the forms of oxyanions and organometalloids. However, the exact chemical speciation of the metalloid to which living organisms are exposed is still unknown [1]. In solution at physiological pH, Te^{IV} likely exists in the form of $HTeO_3^-/TeO_3^{2-}$ at a ratio of ~100:1. Thus, the standard redox

potential of the Te/TeO_3^{2-} couple (0.42 V) at basic pHs, would raise to 0.12 V for the couple $HTeO_3^{-}/TeO_3^{2-}$ at pH 7.0 [2]. Interestingly, tellurate (TeO_4^{2-}) and tellurite (TeO_3^{2-}) oxyan- ions can serve as electron acceptors in the respiratory chain of certain bacteria hence sustaining anaerobic growth [3,4]. In the past, periplasmic and membrane bound nitrate reductases from *Escherichia coli, Ralstonia eutropha, Paracoccus denitrificans*, *Para- coccus pantotrophus* and *Rhodobacter sphaeroides* have shown the capacity to reduce tellurite *in vitro* [5,6]. TeO_3^{2-} reduction and precipitation, in the form of metal Te^0, takes place either in the cyto- plasmic space, which necessitates a mechanism of tellurite entry into cells, or externally to cells, *e.g.*, cell surface and/or periplas- mic space [7]. Exogenous Te° deposits are particularly evident in those species, such as *Sulfurospirillum barnesii* and *Bacillus bev- eridgei*, able to use tellurite and tellurate as exogenous electron acceptors under anaerobic respiration conditions [4]. However, also other species such as *Pseudomonas aeruginosa*, *E. coli*, *Erwinia caro- tovora* and *Agrobacterium tumefaciens* accumulate Te^0 deposits in the periplasmic space, that is, outside the cytoplasm [8].

Tellurite reduction to crystal particles of elemental Te^0 were reported either inside or outside the cells of bacterial species such as *Rhodobacter capsulatus* [9], *R. sphaeroides* [10], *Pseudomonas pseudoalcaligenes* KF707 [2], Strain ER-Te-48 [3], *S. barnesii* [11], *Bacillus selenitireducens* [4]. It is noteworthy that the extracellu- lar production of nanoprecipitates has wider applications than intracellular accumulation. One interesting example is the case of biopalladium particles accumulated on the cell wall of the iron reducer *Shewanella oneidensis* MR-1 used *in vivo* as catalysts in the dechlorination of polychlorinated biphenyl (PCBs) [12].

Presently there are no reports on the catalytic use of exoge- nously generated Te^0 nanoparticles by microorganisms; however, the physical properties of this metalloid do not exclude *a pri- ori* this possibility as telluro-compounds are increasingly used as catalysts [13]. Indeed, unlike bulk material, nanoparticles show peculiar physical, chemical, electronic and biological properties that derive from their size and are due to their large surface to volume ratio, large surface energy, spatial confinement and reduced imperfections. Although chemical methods for the pro- duction of nanoparticles are extensively applied [14–16], even at large industry-ready scales [17], they typically involve the use of toxic reactants and organic solvents. This represents a hindrance both from an economic and from an environmental point of view, while also limiting their application in clinical fields. Owing to this, microbiological methods to generate nanoparticles are regarded as safe, cost-effective and environment-friendly processes with a good scale-up potential for industrial production. Their develop- ment and implementation represent a key goal in nanotechnology but remain a challenge as for today. In this respect, it has been shown that quinone-type redox mediators can participate in the biotransformation of azo dyes, nitro aromatics, polychlorinated compounds, Fe^{III} oxides, U^{VI}, Tc^{VII}, As^{V}, Se^{IV} and Te^{IV} [18–20].

Facultative phototrophic microorganisms of the genus *Rhodobacter* are extensively studied and genetically tractable [1], which allows the ready use of genetic engineering

and molec- ular biology. We have recently reported that photosynthetic cells of *R. capsulatus* grown in the presence of lawsone (2-hydroxy- 1,4-naphthoquinone), catalyze the extracellular accumulation of Te^0 nanoprecipitates (hereafter named: TeNPs) in contrast to the formation of intracellular deposits seen in the absence of lawsone [21]. Surprisingly, other quinone analogues such as menadione (2-methyl-1, 4-naphthoquinone) or juglone (5-hydroxy-1,4- naphthoquinone) had a minor effect on extracellular production of TeNPs. Another interesting observation was that production of these extracellular particles depended to the carbon source used for cell growth [21].

To better understand the role of both carbon sources and law- sone in controlling the formation of TeNPs, we studied in details the growth conditions allowing photosynthetic grown cells of *R. capsulatus* to reduce exogenously the toxic oxyanion tellurite to tellurium nanoparticles. Here we report the characterization of the cultural conditions to generate TeNPs as a function of var- ious carbon sources, lawsone concentration, amount of tellurite and nanoparticles generation times. The utilization of live bacterial cultures along with the possibility of manipulating TeNPs' charac- teristics by changing the growth conditions, represent an important novelty relative to previous works [20,22]. We also present a series of analyses made by atomic force microscopy (AFM), X-ray photo- electron spectroscopy (XPS) and FT-IR analysis (XPS) to define the size and the actual nature of the external organic coating of TeNPs produced under standardized conditions.

Materials and methods

Growth conditions and nanoparticles production

R. capsulatus strains B100 (wild type) and RTE37 (tellurite uptake minus mutant) were grown in *RC*V minimal medium buffered at pH 6.8 [23] under anaerobic photosynthetic conditions with different carbon sources as specified in Section 3.1. The cells suspensions were then diluted 1:10 in a filled screw-capped tubes containing fresh growth medium, with the same carbon source of the starting culture, and anaerobiosis was obtained upon incuba- tion for 20 h in the dark, to allow for the complete O_2 consumption by cell respiration [24]. After reaching anaerobiosis, K_2TeO_3 was added at a concentration of 1 mM and lawsone was added routinely at a concentration of 25 μM, or at the concentrations specified in Section 3.2, and the tubes were put in the light (200 W/m^2). At the end of this procedure, it was estimated that the redox potential of the growth medium was below 110 mV since the redox indicator resazurin (2 μgr/ml) was totally colorless [24]. All different carbon sources used in the growth experiments were added at a concen- tration of 30 mM except for the pyruvate experiments described in Section 3.1.

The TeNPs were prepared after incubation of the microbial cultures in the light for 24, 120 and 240 h. The cultures were cen- trifuged first at 27,200 *g* for 20 min in order to collect the cells. The obtained supernatant was centrifuged in a bench minifuge at the maximum speed for 30 min and the collected nanoparticles were washed twice in Milllipore purified water. The TeNPs were quantified (total yield) on a Jasco V -550

spectrophotometer at the maximum absorbance peak (550 nm). The TeNPs production was normalized to the biomass by dividing the value of the maximum absorbance peak for the biomass expressed as mg of proteins per ml of culture (normalized yield).

Biochemical methods

The quantitative determination of potassium tellurite in liquid media was done using the reagent diethyldithiocarbamate (DDTC) (Sigma) as described by Turner et al. [25].

Protein content of whole cells was determined by the method of Lowry et al. [26] after one-minute incubation with 0.1 N NaOH in boiling water. Crystalline bovine serum albumin (Sigma) was used as the protein standard.

Atomic force microscopy imaging and morphometry

To characterize the morphology of TeNPs, 5 µl aliquots of puri- fied suspensions were diluted (10x) with 45 µl of ultrapure water and left to equilibrate at room temperature for 10 min. 10 µl of the diluted sample were then deposited on freshly cleaved mica (RubyRed Mica Sheets, Electron Microscopy Sciences, Fort Wash- ington, USA) and left to adsorb for 5 min. The sample was then rinsed with 400 µl of ultrapure water and dried with a gentle nitrogen flow. AFM imaging was performed on a Multimode 8 microscope equipped with a Nanoscope V controller and a type J piezoelectric scanner (Bruker, USA). Samples were scanned in air using Peak Force Tapping mode with Scanasyst-Air probes (Bruker, USA). We took special care to obtain images in which the met- alloid nanoparticles appeared well spread and isolated on the surface rather than overlapped and tangled. Raw images were processed to remove background nonlinearity using Gwyddion v2.40 (http://gwyddion.net/). A threshold mask was then used to exclude the flat, empty areas of the images, singling out the aggregates for successive morphometric analysis. TeNPs lengths were evaluated by simply measuring the distance between the two furthest points in the original mask.

first order flattening

X-ray photoelectron spectroscopy (XPS)

XPS analyses were carried out on specimens prepared as detailed in the previous section for AFM measurements by using an Escalab 250Xi (Thermo Fisher Scientific Ltd., UK) equipped with a monochromatic Al Ka excitation source, electron and ion flood guns for charge neutralization and a 6-channeltron detection system. Spectroscopic data were processed with the Avantage v.5 software.

FT-IR spectroscopy

The FT-IR spectrum was recorded on a PerkinElmer Spectrum One FT-IR spectrophotometer equipped with a FR-DTGS detector. The sample was prepared by grounding in an agate mortar 1 mg of TeNPs with 100 mg of dry potassium bromide. The powder was pressed at 10 t/cm^2 and the resulting disc was analyzed using the transmittance mode. A blank KBr disc was used as background and 100 scans, at a

resolution of 1 cm^{-1}, were averaged.

Results

How the carbon source affects TeNPs formation

In *R. capsulatus* the production of extracellular TeNPs requires anaerobic growth conditions and, as previously shown [21], is associated to the presence of the redox mediator lawsone (2- hydroxy-1,4-naphthoquinone). The strict dependence of tellurite reduction on the presence of a metabolizable carbon source was proven by incubating *R. capsulatus* cells in the presence of 0.5 mM tellurite and 4 mM pyruvate, which represents a limiting concen- tration able to sustain the complete reduction of the oxyanion over a 24 h period (not shown).

Fig. 1 shows two parallel cultures subjected to different growth regimes. The first culture received 0.5 mM tellurite (full arrow), with no additional carbon source, at time 0, 24 and 48 h. The initial reduction of tellurite is dependent on the residual pyruvate from the inoculum (Fig. 1A). To the second culture were added both tel- lurite 0.5 mM and pyruvate 4 mM (empty arrow) at time 0, 24 and 48 h (Fig. 1B). By comparing the traces in Fig. 1, it is evident that tellurite reduction takes place only in the presence of pyruvate, *i.e.*, in cells metabolically active.

It has been shown that *R. capsulatus* cells grown with differ- ent carbon sources show different proficiencies in producing TeNPs [21]. Early studies have also demonstrated that tellurite toxicity to cells is strictly related with their capacity to take up the oxyanion into the cytosol *via* the acetate transport system ActP2 in a sort of "suicide mechanism" [1]. Having shown that TeNPs production requires metabolically active cells [21], different carbon sources were tested for TeNPs production in light of their influence on tel- lurite toxicity on cells of *R. capsulatus* B100 (w.t.). As reported in Table 1, pyruvate and lactate, previously shown to limit the entry of tellurite by competing for the same carrier, *i.e.*, ActP2 [27], were the best carbon sources for TeNPs production. Fructose, which deter- mines a moderate tellurite uptake by inducing a lower expression of the transporter ActP2 [28], concurrently allowed an intermediate TeNPs yield. Finally, malate, which has no protective action against tellurite with the highest uptake rate in *R. capsulatus* [27], showed no TeNPs production.

To relate the production of TeNPs to the level of tellurite uptake more conclusively, *R. capsulatus* RTE37, one of a series of tellu- rite uptake minus mutants previously isolated [29], was tested. As shown in Table 1, RTE37 mutant behaves like the wild type B100 when pyruvate is the carbon source. More interestingly, when malate is the growth substrate, RTE37 still produces high amounts of TeNPs in sharp contrast to the wild type. Overall, these results support the concept that tellurite uptake activity is a key factor in determining extracytosolic TeNPs production by *R. capsulatus*.

For a more quantitative analysis of the microbial response to the different cultural conditions that lead to TeNPs production, the nanoparticles yields were related to the biomass (total proteins) measured at the end of the incubation period. As seen in Table 1, cells incubated with fructose increased significantly their normal- ized yield relative to

the total yield, while there was no significant change for the other carbon sources. The change with fructose is due to a lower biomass produced over the incubation period. As men- tioned above, the intermediate tellurite uptake allowed by fructose also produces an intermediate toxic effect that restrains the cells from full growth and, as a consequence, from maximal TeNPs pro- duction.

How lawsone concentration affects TeNPs formation

The redox mediator lawsone, albeit essential for the produc- tion of external nanoparticles, is toxic to cells when added at concentrations $\geq$ 50 µM, although cell growth is seen also with

0.2 mM lawsone [21]. Therefore, the determination of the lowest lawsone concentration still able to promote a massive production of TeNPs is an important step for the optimization of a micro- biological approach. Nanoparticles were prepared, following the standard procedure outlined in 2.1, in the presence of 5, 10 and 25 µM lawsone. As shown in Table 2, at lawsone 10 and 25 µM the TeNPs yield is not significantly different, while it is less than half at 5 µM. The yield normalized for the biomass (mg prot/ml of culture) does not change, because the cultures behave equally well at the three lawsone concentrations, indicating that these conditions do not affect cellular growth. These results set at 10 µM lawsone the minimal concentration required for maximum yield under the growth conditions described.

Atomic force microscopy (AFM) analysis of the TeNPs showed that increasing concentration of the mediator lawsone had a direct effect on the average length and size distribution of the extra- cellular TeNPs produced (Fig. 2). The predominance of longer nanoparticles at higher lawsone concentrations (between 10 and 25 µM) may be due to the kinetics of elongation for which sub-saturating concentrations of the mediator could be limiting. On one hand, this findings call for further caution on the best compromise between yield and toxicity to the cell, as they both depend on lawsone concentration, on the other hand, they open to the possibility of defining suitable cultural conditions for manipu- lating the nanoparticles' size.

In order to overcome this limitation, tellurite concentration opti- mal for extracellular NPs productions was first determined, and it was found that photosynthetic cultures completely reduced tellu- rite 1 mM to Te^0 in less than 24 h, in the presence of 25 µM lawsone and 30 mM pyruvate. Therefore, to test the response of the cells to higher concentrations, the toxicity limitation was circumvented by adding tellurite daily at a concentration of 1 mM with pyruvate replenished every 4 days over a 10 days period. This regime led to the accumulation of progressively larger tellurite nanoparticles up to 600–700 nm in length (Fig. 3). The size distribution of the TeNPs, which widens over the incubation period, is a good indication that accretion of the already formed TeNPs is an ongoing process over the entire experimental period, and it is paralleled by continuing initiation of new ones. Two different mechanisms could explain this scenario, namely: (i) either the same cell starts the formation of new TeNPs as the longer ones detach, possibly as a mere consequences of mechanical shearing forces, or (ii) subpopulations of cells initiate the formation process independently at different times.

TeNPs outer coating

TeNPs were probed by X-ray photoelectron spectroscopy (XPS). The XPS analysis revealed the presence of C, O and N, which is indicative of organic material that is likely responsible for keep- ing the particles in solution in aqueous solvents. The C 1s signal is characterized by three components, localized at Binding Energy (BE) 285.0 eV, 286.2 eV and 288.0 eV and assigned to C C, C O and COO groups, respectively. N 1s peak at BE 400.0 eV was assigned to the amine group. Al and K signals refer to chem- ical species present during sample preparation. The Te 3d signal was characterized by the typical spin-orbit doublet Te $3d_{5/2}$ and Te $3d_{3/2}$, separated by 10 eV (Fig. 4). The peak-fitting routine applied to the Te $3d_{5/2}$ signal showed the presence of 2 peaks at BE 573.1 eV and 576.4 eV, assigned to metallic and oxidized state of tellurium [30]. As the XPS analysis invests mainly few nanometers of the nanoparticles superficial layers, the great abundance of organic material suggests the presence of an external coating.

Discussion

This work examines for first time in detail the capacity of anaerobic photosynthetically grown cultures of *R. capsulatus* to biotransform tellurite oxyanions (TeO_3^{2-}) into elemental Te^0 nanoparticles (TeNPs) as a function of different cultural param- eters: nature of the carbon source, concentration of exogenously added lawsone, amount of tellurite and duration of the incubation period.

As far as the carbon source is concerned, pyruvate and lactate resulted to be the best electron donors for Te° nanoprecipitates in line with the concept that TeNPs production requires metabolically active cells. Indeed, as pyruvate and lactate compete with tellu- rite for the use of the ActP2 permease to entry into cells (see also graphical abstract), these two monocarboxylic acids not only act as substrates but also preserve the cells from tellurite toxicity by limiting the oxyanion entry into cytosol [27]. Accordingly, malate- grown cells of RTE37 mutant (*actP2* minus) generate a consistent amount of TeNPs, in contrast to B100 wild type cells, which are killed by tellurite under these conditions.

The redox mediator lawsone (E_h^{0r} = 145 mV), when used at a concentration <10 μM, affected both kinetics and amount of TeNPs production. Further, growing cultures over a 10 days period with daily additions of 1 mM tellurite with no further addition of law- sone, led to the accumulation of progressively larger TeNPs showing a wide size-range up to 600–700 nm in length. Taken together, these findings suggest that both nucleation of new particles and accretion of already formed ones take place over the entire cell growth period possibly by Ostwald ripening mechanism [32]. As we have shown that the cultural parameters affect both the for- mation kinetics and particles size, it is reasonable to foresee how microbiological manipulations could allow the production of NPs with defined characteristics.

A *prima facie* analysis of the bio-produced TeNPs with XPS and FT-IR spectroscopic techniques indicated the pres- ence of an organic outer coating, as

previously reported in the bioproduction of selenium nanoparticles by *E. coli* [31], which is likely to keep the particles in solution in aqueous solvents. In this respect, there is a significant knowledge gap in understanding the mechanism of bio-formation of metallic NPs so to preclude, at the present research stage, mass production on an industrial scale using bacterially based nano-manufacturing. Bacterial synthesis of NPs is generally achieved by a reduction step followed by a precipitation step with the latest composed of two parts: nucleation and crys- tal growth [33]. To date, only the reduction step has been studied extensively [1,34] whereas the biological processes responsible for nucleation and crystal growth are not fully understood although there is some evidence that proteins might play a key role in the nucleation and crystal growth of bacteriogenic metallic NPs [31]. A bacterial protein – cytochrome *c*3 – was found to reduce selenate (SeO_4^{2-}) in aqueous solution leading to the formation of one- dimensional chain like aggregates of selenium nanoparticles [35]. In magnetosomes of the magnetotactic bacterium *Magnetospiril- lum magneticum* AMB-1, membrane proteins are tightly bound to the magnetic NPs [36–38], and a single protein (Mms6) was shown to control the shape of the final nanomagnetite particles [39]. Similarly, the rate of crystal growth and the morphology of gold (Au) NPs were shown to be controlled by proteins [40,41].

In the graphical abstract, the working hypotheses summariz- ing previous and present results on the TeNPs production by the photosynthetic bacterium *R. capsulatus* are depicted. The biosyn- thesis of TeNPs ouside the cells is likely to involve two steps: (i) the reduction of tellurite to elemental Te^0 mediated by the redox solu- ble carrier, lawsone, and (ii) the subsequent growth of Te^0 crystals into TeNPs possibly *via* the Ostwald ripening mechanism [32,34]. Reduction of tellurite to elemental Te^0 can be carried out intra- cellularly, in the periplasmic space or extracellularly in different microorganisms and thus, the growth of bacterial TeNPs can take place either inside or outside the cell cytosol [3–9,21]. It should be noted that the present study did not distinguish between TeNPs that grew outside the cells by means of the redox mediator law- sone from those which grew into cytosol and then were released in the growth medium by cell lysis (see graphical abstract). However, based on previous results [21], the latter mechanism does not affect significantly the total extracellular TeNPs amount which is almost entirely dependent on the addition of lawsone [21]. An additional aspect to be underlined is that the growth of TeNPs takes place in the presence of an outer organic envelope (this work). It has been reported that the average length of cytosolic Te^0 crystals is in the range of 100 nm in cells harvested after 24–48 h growth [34] while the size of extracellular TeNPs is close to 600–700 nm after 10 days of incubation (this work). Thus, the process of TeNPs lengthening in the presence of an outer organic coating cannot exclude *a pri- ori* an ancillary mechanism consisting of the periplasmic reduction of tellurite by means of the redox mediator lawsone; in this case, Te^0 crystals formed in the periplasmic space could be released into the growth medium in the form of bulges through a process remi- niscent of the outer membrane (OM) vesicles generation [42] (see graphical abstract). Interestingly, SEM images (Fig. S1) of *R. cap- sulatus* cells grown under anaerobic-phototrophic conditions with tellurite *plus* lawsone bring for the first time some support to this latter working hypothesis as they show the presence of "finger-like bulges" protruding from the cell poles.

On the other hand, since the actual nature and function of these cell-bulges is not clear at the moment, the most accredited mechanism for TeNPs formation outside the cells is based on physical and chemical properties of lawsone [20,43], namely: 2-hydroxy-1,4-naphtoquinone is likely to function as an electron redox shuttle [20,21] carrying the reducing equivalents from the membrane-bound electron transport chain (ETP, graphical abstract) to soluble tellurite molecules to allow their precipitation in the form of metallic TeNPs. Further studies aiming to decipher the actual mechanism of bioproduction of TeNPs by *R. caspulatus* are compelling.

Conclusions

1 Pyruvate and lactate, previously shown to limit the entry of tellu- rite into cells of *R. capsulatus* by competing for the same carrier, *i.e.*, acetate permease ActP2, were the best carbon sources for TeNPs production;
2 At lawsone 10 and 25 μM the TeNPs yield does not change signif- icantly, while it is less than half at lawsone 5 μM. It is concluded that 10 μM lawsone is the minimal concentration required for maximum yield under the growth conditions described;
3 Growing cultures with daily additions of 1 mM tellurite led to the accumulation of TeNPs with dimensions from 200 up to 600–700 nm in length as determined by atomic force microscopy (AFM);
4 The size distribution of the TeNPs, which widens over a 10 days growth period, indicated that accretion of the already formed TeNPs was an ongoing process over the entire experimental period, and it was paralleled by continuing initiation of new ones;
5 X-ray photoelectron spectroscopy (XPS) and Fourier transform infrared (FT-IR) analysis of TeNPs indicated they are surrounded by an organic coating that keeps the particles in solution in aque- ous solvents.

References

[1] D. Zannoni, F. Borsetti, J.J. Harrison, R.J. Turner, The bacterial response to the chalcogen metalloids Se and Te, Adv. Microb. Physiol. 53 (2008) 1–71.
[2] G. Di Tomaso, S. Fedi, M. Carnevali, M. Manegatti, C. Taddei, D. Zannoni, The membrane-bound respiratory chain of *Pseudomonas pseudoalcaligenes* KF707 cells grown in the presence or absence of potassium tellurite, Microbiology 148 (2002) 1699–1708.
[3] J.T. Csotonyi, E. Stackebrandt, V. Yurkov, Anaerobic respiration on tellurate and other metalloids in bacteria from hydrothermal vent fields in the eastern Pacific Ocean, Appl. Environ. Microbiol. 72 (2006) 4950–4956.
[4] S.M. Baesman, T.D. Bullen, J. Dewald, D.H. Zhang, S. Curran, F.S. Islam, T.J. Beveridge, R.S. Oremland, Formation of tellurium nanocrystals during anaerobic growth of bacteria that use Te oxyanions as respiratory electron acceptors, Appl. Environ. Microbiol. 73 (2007) 2135–2143.
[5] C. Avazeri, R.J. Turner, J. Pommier, J.H. Weiner, G. Giordano, A. Vermeglio, Tellurite and selenite reductase activity of nitrate reductases from *Escherichia coli*: correlation with tellurite resistance, Microbiology 143 (1997)

1181–1189.
[6] M. Sabaty, C. Avazeri, D. Pignol, A. Vermeglio, Characterization of the reduction of selenate and tellurite by nitrate reductases, Appl. Environ. Microbiol. 67 (2001) 5122–5126.
[7] S.M. Baesman, J.F. Stolz, T.R. Kulp, R.S. Oremland, Enrichment and isolation of *Bacillus beveridgei* sp. nov. a facultative anaerobic haloalkaliphile from Mono Lake. California, that respires oxyanions of tellurium, selenium, and arsenic, Extremophiles 13 (2009) 695–705.
[8] S.M. Trutko, V.K. Akimenko, N.E. Suzina, L.A. Anisimova, M.G. Shlyapnikov,
[9] F. Borsetti, R. Borghese, F. Francia, M.R. Randi, S. Fedi, D. Zannoni, Reduction of potassium tellurite to elemental tellurium and its effect on the plasma membrane redox components of the facultative phototroph *Rhodobacter capsulatus*, Protoplasma 221 (2003)
[10] M.D. Moore, S. Kaplan, Members of the family *Rhodospirillaceae* reduce heavy-metal oxyanions to maintain redox poise during photosynthetic growth, ASM News 60 (1994) 17–24.
[11] R.S. Oremland, M.J. Herbel, J.S. Blum, S. Langley, T.J. Beveridge, P.M. Ajayan, T. Sutto, A.V. Ellis, S. Curran, Structural and spectral features of selenium nanospheres produced by Se-respiring bacteria, Appl. Environ. Microbiol. 70 (2004) 52–60.
[12] D. De Windt, P. Aelterman, W. Verstraete, Bioreductive deposition of palladium (0) nanoparticles on *Shewanella oneidensis* with catalytic activity toward reductive of dechlorination of polychlorinated biphenyls, Environ. Microbiol. 7 (2005) 314–325.
[13] A.B. Powell, S.S. Stahl, Aerobic oxidation of diverse primary alcohols to methyl esters with a readily accessible heterogeneous Pd/Bi/Te catalyst, Org. Lett. 15 (2013) 5072–5075.
[14] S. Zinatloo-Ajabshir, M. Salavati-Niasari, Nanocrystalline Pr_6O_{11}: synthesis characterization, optical and photocatalytic properties, N. J. Chem. 39 (2015) 3948–3955.
[15] F. Beshkari, S. Zinatloo-Ajabshir, M. Salavati-Niasari, Preparation and characterization of the $CuCr_2O_4$ nanostructures via a new simple route, J. Mater. Sci.: Mater. Electron. 26 (2015) 5043–5051.
[16] S. Zinatloo-Ajabshir, M. Salavati-Niasari, Preparation and characterization of nanocrystalline praseodymium oxide via a simple precipitation approach, J. Mater. Sci.: Mater. Electron. 26 (2015) 5812–5821.
[17] C.A. Charitidis, P. Georgiou, M.A. Koklioti, A.-F. Trompeta, V. Markakis, Manufacturing nanomaterials: from research to industry, Manuf. Rev. 1 (2014) 11.
[18] B. Zhang, W.Y. Hou, X.C. Ye, S.Q. Fu, Y. Xie, 1D tellurium nanostructures: photothermally assisted morphology-controlled synthesis and applications in preparing functional nanoscale materials, Adv. Funct. Mater. 17 (2007) 486–492.
[19] Z. Lu, C.M. Li, H. Bao, Y. Qiao, Y. Toh, X. Yang, Mechanism of antimicrobial activity of CdTe quantum dots, Langmuir 24 (2008) 5445–5452.

[20] X. Wang, G. Liu, J. Zhou, J. Wang, R. Jin, H. Lv, Quinone-mediated reduction of selenite and tellurite by *Escherichia coli*, Bioresour. Technol. 102 (2011) 3268–3271.
[21] R. Borghese, C. Baccolini, F. Francia, P. Sabatino, R.J. Turner, D. Zannoni, Reduction of chalcogen oxyanions and generation of nanoparticles by the photosynthetic bacterium *Rhodobacter capsulatus*, J. Hazard. Mater. 269 (2014) 24–30.
[22] D.-H. Kim, R.A. Kanaly, H.-G. Hur, Biological accumulation of tellurium nanorod structures via reduction of tellurite by *Shewanella oneidensis* MR-1, Bioresour. Technol. 125 (2012) 127–131.
[23] P.F. Weaver, J.D. Wall, H. Gest, Characterization of *Rhodopseudomonas capsulata*, Arch. Microbiol. 105 (1975) 207–216.
[24] R. Borghese, F. Borsetti, P. Foladori, G. Ziglio, D. Zannoni, Effects of the metalloid oxyanion tellurite (TeO_3^{2-}) on growth characteristics of the phototrophic bacterium *Rhodobacter capsulatus*, Appl. Environ. Microbiol. 70 (2004) 6595–6602.
[25] R.J. Turner, J.H. Weiner, D.E. Taylor, Use of diethyldithiocarbamate for quantitative determination of tellurite uptake by bacteria, Anal. Biochem. 204 (1992) 292–295.
[26] O.H. Lowry, N.J. Rosebrough, A.L. Farr, R.J. Randall, Protein measurement with the folin phenol reagent, J. Biol. Chem. 193 (1951) 265–275.
[27] R. Borghese, D. Marchetti, D. Zannoni, The highly toxic oxyanion tellurite (TeO_3^{2-}) enters the phototrophic bacterium *Rhodobacter capsulatus* via an as yet uncharacterized monocarboxylate transport system, Arch. Microbiol. 189 (2008) 93–100.
[28] R. Borghese, S. Cicerano, D. Zannoni, Fructose increases the resistance of *Rhodobacter capsulatus* to the toxic oxyanion tellurite through repression of acetate permease (ActP), Antonie Van Leeuwenhoek 100 (2011) 655–658.
[29] R. Borghese, D. Zannoni, Acetate permease (ActP) is responsible for tellurite (TeO_3^{2-}) uptake and resistance in cells of the facultative phototroph *Rhodobacter capsulatus*, Appl. Environ. Microbiol. 76 (2010)
[30] A. Bellucci, E. Cappelli, S. Orlando, L. Medici, A. Mezzi, S. Kaciulis, R. Polini, D.M. Trucchi, Fs-pulsed laser deposition of Pb Te and Pb Te/Ag thermoelectric thin films, Appl. Phys. A: Mater. Sci. Process. 117 (2014) 401–407.
[31] R. Jain, N. Jordan, S. Weiss, H. Foerstendorf, K. Heim, R. Kacker, R. Hübner, H. Kramer, E.D. van Hullebusch, F. Farges, P.N.L. Lens, Extracellular polymeric substances govern the surface charge of biogenic elemental selenium nanoparticles, Environ. Sci. Technol. 49 (2015) 1713–1720.
[32] W. Zhang, Z. Chen, H. Liu, L. Zhang, P. Gao, D. Li, Biosynthesis and structural characteristics of selenium nanoparticles by *Pseudomonas alcaliphila*, Colloid Surf. B 88 (2011) 196–201.
[33] C.I. Pearce, V.S. Coker, J.M. Charnock, R.A.D. Pattrick, J.F.W. Mosselmans, N. Law, T.J. Beveridge, J.R. Lloyd, Microbial manufacture of chalcogenide-based

nanoparticles via the reduction of selenite using *Veillonella atypica*: an in situ EXAFS study, Nanotechnology 19 (2008) 155603.
[34] R.J. Turner, R. Borghese, D. Zannoni, Microbial processing of tellurium as a tool in biotechnology, Biotechnol. Adv. 30 (2012) 954–963.
[35] A. Abdelouas, W.L. Gong, W. Lutze, J.A. Shelnutt, R. Franco, I. Moura, Using cytochrome c3 to make selenium nanowires, Chem. Mater. 12 (2000) 1510–1512.
[36] Y.A. Gorby, T.J. Beveridge, R.P. Blakemore, Characterization of the bacterial magnetosome membrane, J. Bacteriol. 170 (1988) 834–841.
[37] W. Leinfelder, K. Forchhammer, F. Zinoni, G. Sawers, M.A. Mandrand-Berthelot, A. Bock, *Escherichia coli* genes whose products are involved in selenium metabolism, J. Bacteriol. 170 (1988) 540–546.
[38] M. Tanaka, Y. Okamura, A. Arakaki, T. Tanaka, H. Takeyama, T. Matsunaga, Origin of magnetosome membrane: proteomic analysis of magnetosome membrane and comparison with cytoplasmic membrane, Proteomics 6 (2006) 5234–5247.
[39] A. Arakaki, J. Webb, T. Matsunaga, A novel protein tightly bound to bacterial magnetic particles in *Magnetospirillum magneticum* strain AMB-1, J. Biol. Chem. 278 (2003) 8745–8750.
[40] S. Brown, Engineered iron oxide-adhesion mutants of the *Escherichia coli* phage lambda receptor, Proc. Natl. Acad. Sci. U. S. A. 89 (1992) 8651–8655.
[41] S. Brown, M. Sarikaya, E. Johnson, A genetic analysis of crystal growth, J. Mol. Biol. 299 (2000) 725–735.
[42] B. György, T.G. Szabó, M. Pásztói, Z. Pál, P. Misják, B. Aradi, V. László, É. Pállinger, E. Pap, Á. Kittel, G. Nagy, A. Falus, E.I. Buzás, Membrane vesicles: current state-of-the-art: emerging role of extracellular vesicles, Cell. Mol. Life Sci. 68 (2011) 2667–2688.
[43] R. Inagaki, M. Ninomiya, K. Tanaka, M. Kaketsu, Synthesis characterization, and antileukemic properties of naphthoquinone derivatives of lawsone, Chem. Med. Chem. 10 (2015) 1413–1423.
[44] M. Kačuráková, N. Wellner, A. Ebringerová, Z. Hromádková, R.H. Wilson, P.S. Belton, Characterisation of xylan-type polysaccharides and associated cell wall components by FT-IR and FT-Raman spectroscopies, Food Hydrocoll. 13 (1999) 35–41.
[45] L.G. Thygesen, M.M. Løkke, E. Micklander, S.B. Engelsen, Vibrational microspectroscopy of food Raman vs. FT-IR, Trends Food Sci. Technol. 14 (2003) 50–57.
[46] K. Maquelin, C. Kirschner, L.-P. Choo-Smith, N. van den Braak, H.P. Endtz, D. Naumann, G.J. Puppels, Identification of medically relevant microorganisms by vibrational spectroscopy, J. Microbiol. Methods 51 (2002) 255–271.
[47] L.L. Wang, L.F. Wang, X.M. Ren, X.D. Ye, W.W. Li, S.J. Yuan, M. Sun, G.P. Sheng,
H.Q. Yu, X.K. Wang, pH dependence of structure and surface properties of microbial EPS, Environ. Sci. Technol. 46 (2012) 737–744.
[48] C. Xu, S. Zhang, C. Chuang, E.J. Miller, K.A. Schwehr, P.H. Santschi, Chemical

composition and relative hydrophobicity of microbial exopolymeric substances (EPS) isolated by anion exchange chromatography and their actinide-binding affinities, Mar. Chem. 126 (2011)

Figure 1

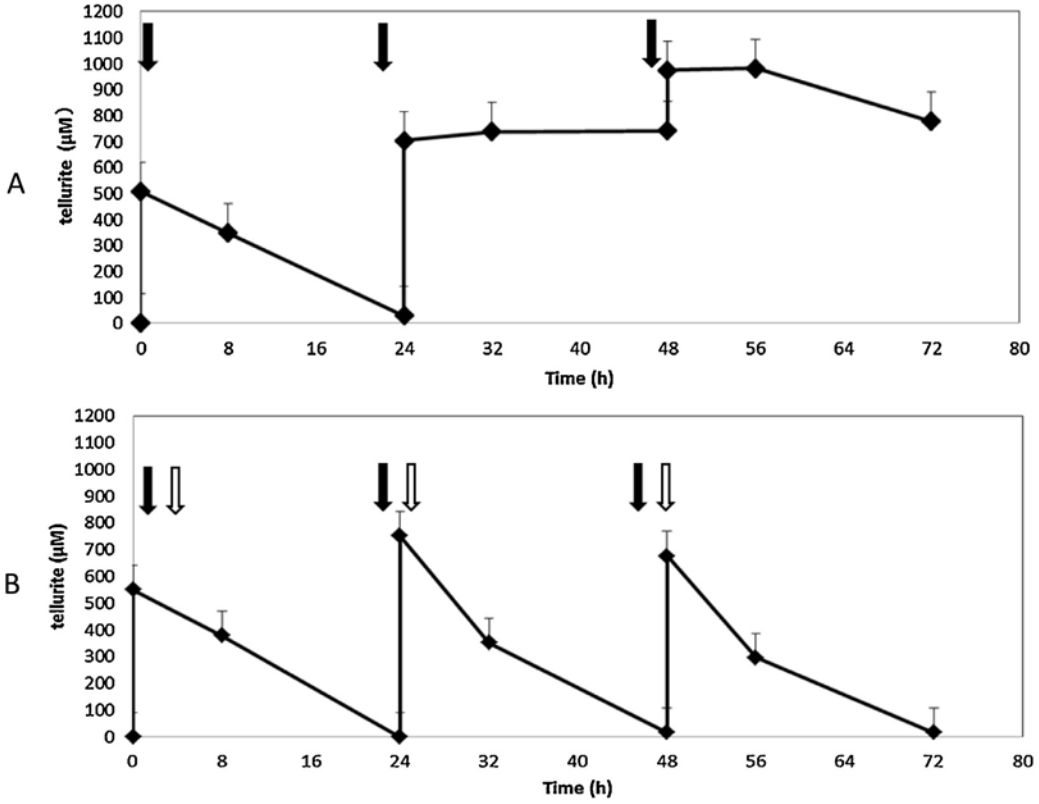
A
tellurite (µM)
1200
1100
1000
900
800
700
600
500
400
300
200
100
0
0
8
16
24
32
40
48
56
64
72
80
Time (h)
B
tellurite (µM)
1200
1100
1000
900
800
700
600
500
400
300
200
100
0
0
8
16
24
32
40
48
56
64
72
80
Time (h)

Figure 2

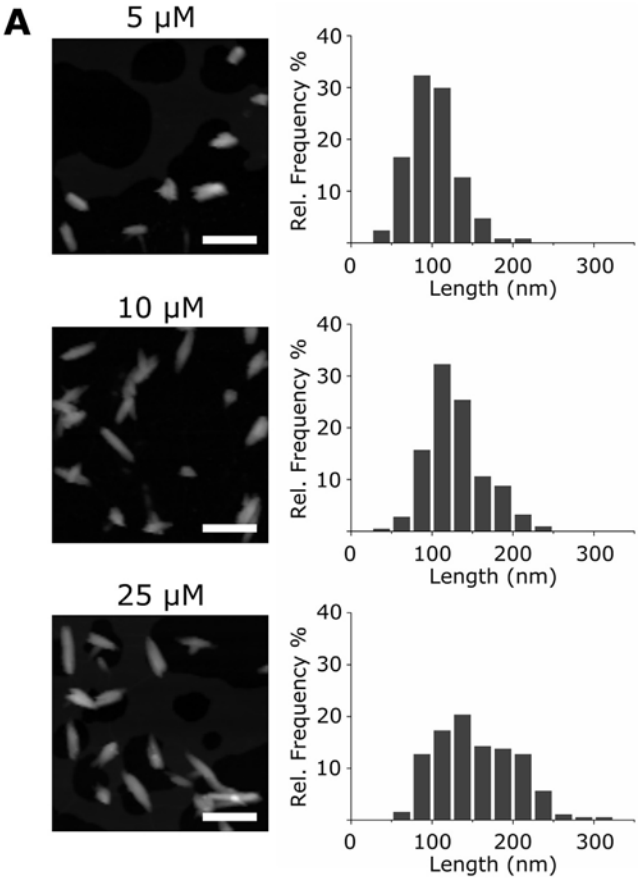
A
5 μM
10 μM
25 μM
Rel. Frequency %
Length (nm)
0
100
200
300
10
20
30
40
B
Length (nm)
250
150
50
0
10
20
30
Lawsone concentration (μM)

Figure 3

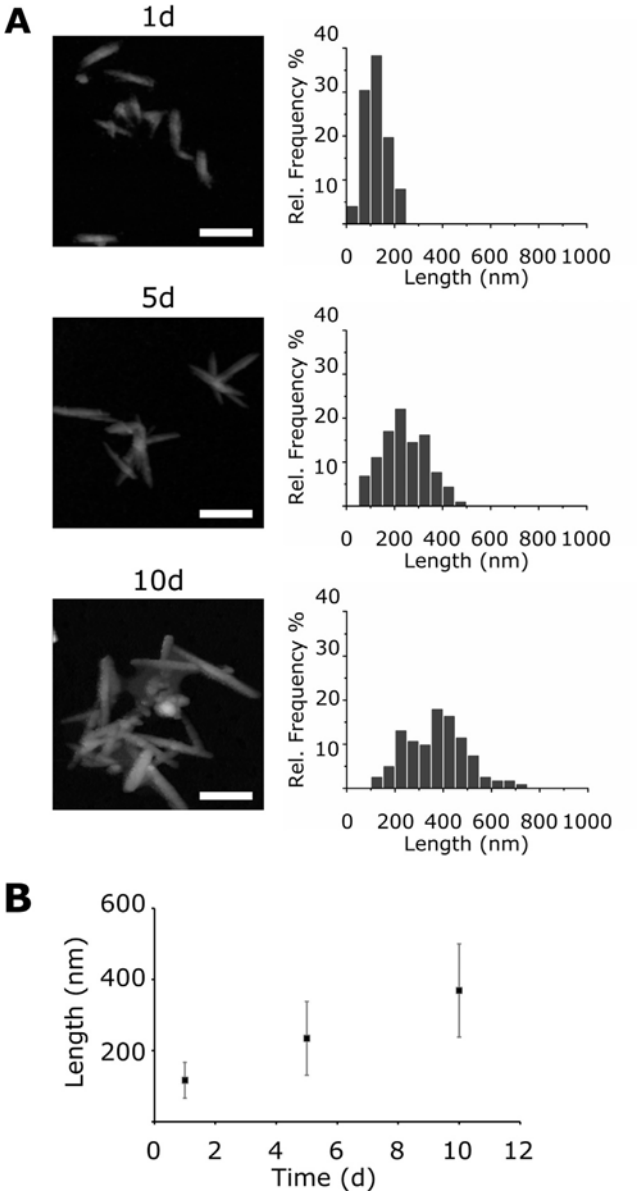
A
1d
5d
10d
Rel. Frequency %
40
30
20
10
0 200 400 600 800 1000
Length (nm)
B
Length (nm)
600
400
200
0 2 4 6 8 10 12
Time (d)

Figure 4

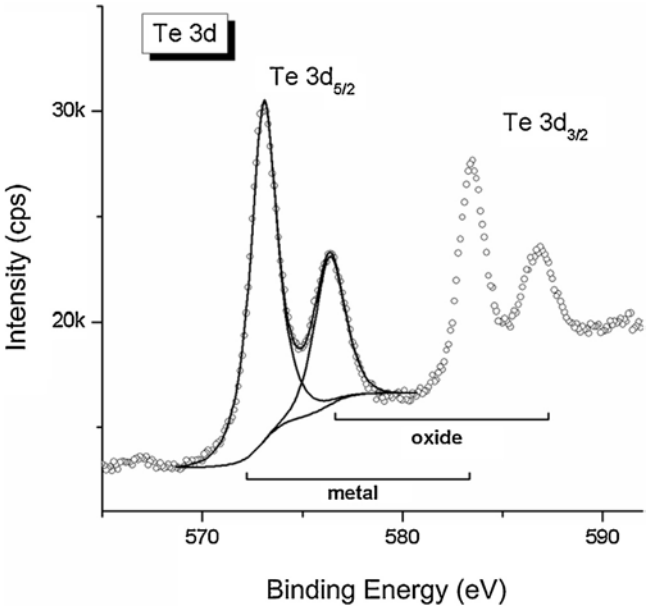

Figure 5

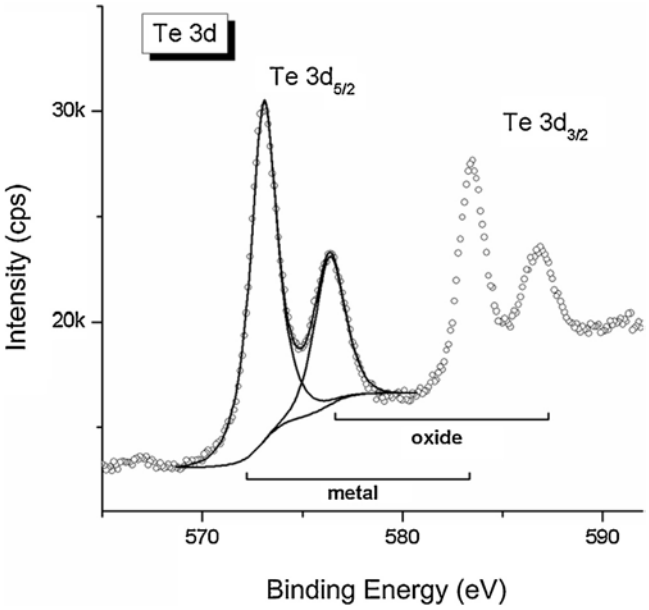

Table 1

Carbon source	B100 (w.t.)				RTE37 (TeO_3^{2-}uptake−)	
	Malate	Pyruvate	Lactate	Fructose	Malate	Pyruvate
Nanoparticles[a] (total yield)	ND[c]	1	1.4	0.3	1.7	1.1
Nanoparticles[b](normalized yield)	ND	1	1.6	1.1	1.9	1

[a] Measured as maximum absorbance peak.

[b] Maximum absorbance peak/mg protein/ml bacterial culture.

[c] Not detectable.

Table 2

Lawsone concentration (μM)	25	10	5
Nanoparticles[a]	1	1.1	0.4
Nanoparticles/mg prot[b]	1	1.1	0.4

[a] Measured as maximum absorbance peak.

[b] Maximum absorbance peak/mg protein/ml bacterial culture.

Table 3 (left)

Name	Peak BE	Atomic %	Assignment
C1s - 1	285.0	26.2	C-C
C1s - 2	286.2	5.7	CO
C1s - 3	288.0	2.6	COO^{-}
$Al2p_{3/2}$	74.3	12.8	Al^{3+}
$K2p_{3/2}$	293.2	2.7	K^{+}
N1s	400.0	1.8	Amine
O1s	531.8	44.1	Oxides
$Te3d_{5/2}$ - met	573.1	2.8	Metallic
$Te3d_{5/2}$ - ox	576.4	1.3	Oxide

Table 4 (right)

Wavenumber (cm^{-1})	Intensity[a]	Assignment[b]	Ref.
3434	s	υ(OH)	[44,45]
3218	s	υ(NH)amideA	[46]
2923	w	$υ_{as}$(CH)	[44]
2852	w	$υ_{s}$(CH)	[44]
1721	w	υ(CO)carbonicacid	[46]
1633	m	υ(CO)amidel	[47,48]
1525	w	δ(NH) amide II	[46]
1408	s	υ(CO)ofCOO^{-}	[46]
1384	m	δ (OH, CH)	[44]
1215	sh	$υ_{as}$(PO)ofPO_2^{-}	[46,47]
1138	sh	υ(COC)inpolysaccharide	[48]
1099	m	υ(CO),υ(CC)	[44,45]
1079	sh	$υ_{s}$(PO)ofPO_2^{-}	[46]
1057	sh	def(COC) in polysaccharide	[47]